I. Sikic, S. Dembele, J. Wen (2018), Non-grey radiative heat transfer modelling in LES-CFD simulated methanol pool fires, Journal of Quantitative Spectroscopy and Radiative Transfer (to be accepted subject to minor revision).

NON-GREY RADIATIVE HEAT TRANSFER MODELLING IN LES-CFD SIMULATED METHANOL POOL FIRES

Ivan Sikic[1], Siaka Dembele[2] and Jennifer Wen[1]*

[1]Warwick FIRE, University of Warwick, Coventry CV4 7AL, United Kingdom
[2]Departmentof Mechanical and Automotive Engineering, Kingston University London, London SW15 3DW, United Kingdom
[*]Corresponding Author: Jennifer.Wen@warwick.ac.uk

ABSTRACT: Non-grey radiation modelling of gas-phase combustion products is performed during runtime of large eddy simulations (LES) of 30cm, 20kW methanol pool fires, based on the experiments of Klassen and Gore (1992) and Weckman and Strong (1996). FireFOAM, the turbulent flame solver part of open source CFD platform OpenFOAM®, was modified to include a new array of gas radiation models. Two grey and three non-grey implementations of the weighted-sum-of-grey-gases (WSGG) are compared in terms of both accuracy and CPU efficiency, along with a 'box' model based on the exponential wide band model (EWB) but specially optimised for fire scenarios. Turbulence-radiation interactions (TRI) are taken into account for the self-correlation of temperature in the emission term of the radiative transfer equation (RTE). Non-grey WSGG models consistently performed better than their grey counterparts, but the two newer WSGG correlations based on up-to-date spectral databases did not perform noticeably better or worse than the older WSGG model, which is a departure from other studies in oxy-fuel conditions. The work also showed that TRI is very important for the accurate prediction of the pool surface radiant feedback and the total radiant output. Some recommendations are made for the fire and radiation community.

KEYWORDS: CFD; radiative heat transfer; turbulent pool fire; FireFOAM; box model; weighted-sum-of-gray-gases

Nomenclature

a	WSGG weighting coefficient
C	Constant for modelling of subgrid temperature fluctuation
C_{TRI}	Turbulence-radiation interaction constant
G	total incident radiation (W/m^2)
h_s	specific enthalpy (J/kg)
I	total radiative intensity (W/m^2)
k	WSGG pressure-absorption coefficient (m^{-1}.atm^{-1})
P	total pressure (Pa or atm)
Pr	Prandtl number
q'''	chemical heat source term (W/m^3)
q_r''	radiative heat flux (W/m^2)
S	Mean beam or path length (m)

Q	heat release rate
T	temperature (K)
U	velocity (m/s)
Greek	
α	thermal diffusivity (m^2/s)
ε	total emissivity
κ	linear absorption coefficient (m^{-1})
λ	wavelength (μm)
η	wavenumber (cm^{-1})
ν	kinematic viscosity (m^2/s)
ρ	density (kg/m^3)
σ	Stefan-Boltzmann constant ($W/m^2/K^4$)
τ	total transmissivity
Φ	radiative scattering phase function
Ω	solid angle (sr)
Subscript	
λ	wavelength dependency
b	Blackbody
w	water vapour
c	carbon dioxide
i	angular direction
j	spectral band or grey gas

1. Introduction

Thermal radiation in combustion systems with high temperatures is an important mode of energy transport that needs to be considered for both fundamental understanding and implementation in practical combustion systems. In the context of fire applications, thermal radiation plays a crucial role in the coupling of combustion, heat transfer, and fluid dynamics in fires and fire suppression. Radiation can significantly affect the flame temperature, which ultimately affects the yield of combustion products, and hence the concentrations of gaseous species and particulates that influence emission, absorption and scattering of radiation [1-2]. Pool fires, considered in this work, are characterised by buoyant diffusion flames developing over a horizontal fuel surface. They are the most basic type of fires and relevant in many domestic or industrial scenarios [3-4]. At the pool surface, the fuel receives heat from the flame above, influencing the burning rate. A fraction of the feedback heat originates from thermal radiation, which generally increases with both fire size and flame luminosity [5]. Even in pool fires as small as 30cm in diameter, with non-luminous flames (e.g. methanol), radiative feedback represents a large fraction of the energy received by the pool surface [6]. Rigorous modelling of radiative heat transfer mechanisms in pool fires is therefore essential for realistic fire simulations.

For an arbitrary scenario the radiative transfer equation (RTE) must be solved at any position along a line of sight for a given wavenumber, making the solution a five-dimensional problem unless simplifications are assumed. Advanced RTE solution methods such as the

Monte-Carlo ray tracing (MCRT) approach are accurate but too computationally demanding in particular in the context of Computational Fluid Dynamics (CFD). Far less involved than the MCRT, typical RTE solvers used in CFD solvers such as the finite volume method (FVM) or the discrete ordinates method (DOM) describe the electromagnetic wave propagation in terms of solid angles. Faster still approaches are found in the P1 and optically-thin approximations which yield a radiant source term without solving the RTE, but by nature they are not suitable for arbitrary and complex scenarios [7]. Generally, the FVM or DOM solver coupled with a suitable gas/particles absorption-emission model can be a viable compromise for CFD. The challenge, then, is the extreme non-greyness of combustion gases (mainly CO_2, H_2O, CO...) in the thermal radiation range (typically 10^5-10^6 absorption lines between wavenumbers 100 and 100,000 cm^{-1}). For the radiation community, many strategies are available, from the most advanced but CPU prohibitive line by line (LBL) approach, to the very crude grey approximations (spectrally constant absorption coefficient), with the various narrow band, wide band and global models in between. Detailed spectral models such as the statistical narrow band (SNB) or the narrow band correlated-k (NBCK) are accurate enough often to replace LBL data [8-10]. In recent years, radiation researchers have coupled narrow band models with FVM or DOM in CFD codes [11-13] (such couplings are feasible by using a non-correlated solution approximation or a correlated-k method). Such setups were used to perform decoupled radiation-only calculations in either pre-solved or synthetic fires (temperature, gas concentrations, etc. reconstructed from empirical correlations), but such models would be too slow to be used during an actual fire simulation and would not capture the real dynamics of the fire. Although comparatively coarse, even the wide band models are slow in their spectral form and have been scarcely used over the years for fire simulations [14-16]. Global models such as the weighted-sum-of-grey-gases (WSGG), Spectral-Line-Based Weighted-Sum-of-Gray-Gases (SLW) or full spectrum correlated-k (FSCK) remain potentially more convenient for CFD engineers, as well as grey approximations. In the WSGG, the real gas absorption properties are replaced with those of fictitious grey gases to approximate the total emissivity or total absorptivity of the real gas. Since the method was pioneered by Hottel and Sarofim [17], many WSGG correlations have been generated for specific problems or to keep up with spectral database updates. A WSGG can be implemented in either banded (one RTE solved for each grey gas) or grey (use of a single absorption coefficient over a mean beam length) fashions. It is the banded WSGG that has attracted the most success from the radiation community, which often dismisses grey approximations as inappropriate for inhomogeneous media [8-10]. However, reference [10] and more recent CFD works from the fire community [18,19] report satisfactory performance in fires where grey emission by soot particles dominates radiation over non-grey combustion gases (a common approximation for moderately-sooting fires e.g. heptane). However, in spite of some of their advantages, global models such as WSGG or FSCK for the gas phase radiation are difficult to couple with another non-grey phase requiring spectral treatment such as liquid water droplets from a fire-suppression spray system. Modelling such a mixture of gases and non-grey droplets usually requires spectral Mie theory modelling and the knowledge of band limits where both phases absorb/emit, which only a spectrally-based band gas model can provide, e.g. the exponential wide band or EWB. CFD modelling of fire suppression systems has been a long sought-after goal of the industry and is being featured in some of the latest

developments of the fire modelling community [20,21], hence a radiation modelling capability for both the gas and non-grey particulate phase has to be the next step.

The main goal of this work is to investigate and make recommendations on the issue of non-grey gas radiation from a CFD fire engineering point of view, with solutions that offer reasonable computational overheads and accuracy and potentially address both single phases (gases only or gases/grey soot mixtures) and two-phases (gases and non-grey particles) problems.

The methodology proposed in this study will be as follows: radiative transfer calculations will be performed simultaneously with LES of pool fires, using an FVM solver and comparing the accuracy (and computing time) of several grey and non-grey gas radiation models against reference experimental works. The software environment is the open source LES-CFD code FireFOAM version 2.2.x, a dedicated turbulent diffusion flame solver developed by FM Global as part of the OpenFOAM C++ toolbox. The pool of diameter 30 cm is fed with methanol (extremely low soot production) in order to enable proper assessment of non-grey gas radiation models without the bias of a grey soot phase. The investigated models are banded and grey implementations of three different WSGG models, and one "box" model (a stepwise-grey version of the EWB), specifically optimised by the authors for fire applications and efficient computing times. The proposed contributions of this work are: i) the comparative analysis of older/original WSGG correlations against newer ones mainly developed for oxy-fuel applications, as to the best knowledge of the authors, these newer models were never assessed in fire applications ; ii) the assessment of an original and CPU-efficient implementation of an EWB-based gas box model that can be eventually coupled with non-grey particulates requiring spectral treatment (e.g. water droplets) ; iii) the investigation of the accuracy and computing times of the gas radiation models in fully coupled LES CFD fire simulations, thus focusing this work towards industrial and engineering applications; rather than using synthetic fires or a decoupled approach as employed in most literature studies.

2. Mathematical modelling and numerical approaches

2.1. Governing equations and numerical methods

FireFOAM-2.2.x solves the sensible enthalpy equation, Eq. (1), in its averaged form suitable for the large eddy simulation (LES) approach. The over-bars and tildes stand for spatial filtering and Favre averaging respectively. The combustion model based on the eddy dissipation concept (EDC) of Magnussen and Hjertager [22] was extended for LES and implemented in FireFOAM by Chen et al. [23,24]. The model uses the concept of energy cascade, from the integral length scale (largest structures containing most of the kinetic energy) down to the Kolmogorov scale of the smallest eddies. Assuming that the LES filter width usually falls between these two scales, the total kinetic energy and its dissipation rate may be derived from subgrid-scale quantities [24]. For the simulated pool fires, the pressure-implicit split operator (PISO) algorithm was used, which is OpenFOAM's iterative procedure for solving the equations of velocity and pressure in transient problems [25].

$$\frac{\partial \bar{\rho}\tilde{h}_s}{\partial t} + \frac{\partial \bar{\rho}\widetilde{u_j}\tilde{h}_s}{\partial x_j} = \frac{D\bar{p}}{Dt} + \frac{\partial}{\partial x_j}\left\{\bar{\rho}\left\{\alpha + \frac{\nu_t}{Pr_t}\right\}\frac{\partial \tilde{h}_s}{\partial x_j}\right\} + \dot{q}''' - \nabla.\dot{q}''_r \quad (1)$$

In Eq. (1), $\nabla.q''_r$ is the divergence of the radiative flux (radiative source term or radiative power dissipated per unit volume), coupling the radiant energy with the conservation of total energy. At a spatial location $\boldsymbol{x}$ the radiative source term is expressed as:

$$P_r(\boldsymbol{x}) = -\nabla.\dot{q}''_r = -\int_0^\infty \int_0^{4\pi} \nabla.I_\lambda(\boldsymbol{x},\boldsymbol{s})\boldsymbol{s}d\Omega d\lambda \quad (2)$$

The monochromatic radiant intensity is the solution of the radiative transfer equation (RTE). In its non-scattering form (applicable to gas phases), the spectral RTE takes the form

$$\boldsymbol{s}.\nabla I_\lambda(\boldsymbol{s},\boldsymbol{x}) = \kappa_\lambda(I_{b,\lambda}(T) - I_\lambda(\boldsymbol{s},\boldsymbol{x})) \quad (3)$$

The radiative source term defined in Eq. (2) may now be rewritten as:

$$\nabla.\dot{q}''_r = \int_0^\infty \kappa_\lambda\left(4\pi I_{b,\lambda} - \int_0^{4\pi} I_\lambda d\Omega\right)d\lambda \quad (4)$$

The total radiant power dissipated by a source can be obtained by a volume integration of the source term, but also by a surface integration of the flux, since the flux must verify the divergence theorem. FireFOAM's built-in FVM solves Eq. (2) by integration over the cell volume and the solid angle with an upwind scheme. To be able to deal with multi-dimensional problems without resorting to a ray tracing type method, the RTE solution method is uncorrelated, i.e. along a line of sight, the history of the intensity is retained from the previous cell.

2.2. Turbulence-radiation interaction (TRI)

TRI should be taken into account, as per recommendations from various sources such as [11,12,19,40,41]. As detailed by Snegirev in [41], the expansion of the radiant emission term yields a temperature self correlation and a correlation between the filtered absorption coefficient and temperature. Ignoring the higher orders of the expansion, the TRI correlations are summarised as per Eq. (5a) to Eq. (5c).

$$\widetilde{\kappa T^4} = \tilde{\kappa}\tilde{T}^4\left(R_{T^4} + R_{I_b}\right) \quad (5a)$$

$$R_{T^4} \approx \left(1 + 6C_{TRI}\frac{\widetilde{T''^2}}{\tilde{T}^2}\right) \quad (5b)$$

$$R_{I_b} \sim \frac{\widetilde{T''^2}}{\tilde{\kappa}\tilde{T}}\frac{\partial \kappa}{\partial T}\bigg|_{\tilde{T}} \quad (5c)$$

Where the double prime subscript stands for the modelled, subgrid quantity as in [19]. The term R_{I_b} is expected to have a small magnitude [41] and is neglected as in [19] where a moderately-sooting heptane fire was simulated with FireFOAM. Due to its extremely low soot levels a methanol fire is expected to be optically thinner than a heptane fire of similar size, which justifies the sole modelling of R_T^4. A so-called turbulent flame sheet temperature $T_f \equiv \left(\widetilde{T^4}\right)^{1/4}$ [19] is used in the emission terms of Eq. (3) and Eq. (4). It also appears in WSGG calculations (the temperature-dependent weighting coefficients, see 2.3) and in box model routines (Eq. 17-19). The subgrid temperature fluctuation is estimated similarly to [19] i.e.:

$$\widetilde{T''^2} = C\Delta^2\left|\vec{\nabla}\tilde{T}\right|^2 \quad (6a)$$

The resolved temperature fluctuation, *T'*, is calculated by FireFOAM as the difference between the filtered and time-averaged filtered temperature. As in [19], the RMS temperature is thus $\widetilde{T_{rms}} = \widetilde{T''} + \widetilde{T'}$. (6b)

2.3. Weighted-sum-of-grey-gases

Mathematically simple, the concept of a WSGG is to approximate the total emissivity of a real gas (measured or modelled by any model of sufficient accuracy) with a weighted sum of emissivities of a small number of *J* fictitious grey gases, i.e.

$$\varepsilon(T,S) = 1 - e^{-\kappa S} \approx \sum_{j=0}^{J} a_j(T)\left(1 - e^{-k_j p_a S}\right) \quad (7)$$

a is a temperature-dependent parameter used as a weight for the emission term of the RTE and is pre-tabulated. *k* is a wavelength-independent (hence, grey) pressure-absorption coefficient and p_a is the partial pressure of the participating gas. WSGG correlations sampled from the literature yield the k_j and a_j in more or less direct fashion. For the present study three sets of WSGG correlations were considered: the older model of Smith et al. [26], who obtained their coefficients from an EWB calculation of total emissivity of CO_2 and H_2O; and the more recent models by Cassol et al. [27] and Johansson et al. [28] which were developed for oxy-fuel combustion applications using more recent and up-to-date spectral databases (HITEMP10 and HITRAN92 respectively) combined with SNB models. These models will be referred to as simply "Smith", "Cassol" or "Johansson" in this work. The Cassol model retains the traditional WSGG formulation (one set of k_j and a_j for one particular mixture of CO_2 and H_2O). By contrast the Johansson model is valid for any partial pressure ratio of water vapour/carbon dioxide ratio such as $0.125 < p_w/p_c < 2$ and the grey gas absorption coefficients can account for local variations of that ratio.

The WSGG approach can be implemented in two ways; grey or banded. In the grey version an effective or grey absorption coefficient κ is derived from Eq. (7) (with input of a mean beam length *S*) and calculated locally to be used in the non-scattering RTE:

$$\boldsymbol{s}.\nabla I(\boldsymbol{x},\boldsymbol{s}) = \kappa(\boldsymbol{x})[I_b(T(\boldsymbol{x})) - I(\boldsymbol{x},\boldsymbol{s})] \quad (8)$$

Where $I_b = \sigma T^4/\pi$. The finite volume solution of Eq. (8) yields the total directional intensity which is integrated over the solid angle to yield the total incident radiation *G*:

$$G(\boldsymbol{x}) = \int_0^{4\pi} I(\boldsymbol{x},\boldsymbol{s})d\Omega \quad (9)$$

From Eq. (9) the total radiative source term is obtained (where the absorption coefficient and blackbody intensity may vary locally if the gas is inhomogeneous and/or non-isothermal):

$$\nabla.\dot{q}''_r(\boldsymbol{x}) = \kappa(\boldsymbol{x})[4\pi I_b(\boldsymbol{x}) - G(\boldsymbol{x})] \quad (10)$$

The total radiative flux incident to a boundary with normal unit vector $\boldsymbol{n_w}$ is:

$$\dot{q}''_{r,in}(\boldsymbol{x}) = \int_{\boldsymbol{s}.\boldsymbol{n_w}<0} I(\boldsymbol{x},\boldsymbol{s})|\boldsymbol{s}.\boldsymbol{n_w}|d\Omega \quad (11)$$

Alternatively, it was shown in [29] that the RTE may be solved individually for each grey gas, and the total radiant intensity may be reconstructed by simple summation of the grey gas intensities (banded formulation),

$$I(\boldsymbol{x},\boldsymbol{s}) = \sum_{j=0}^{J} I_j(\boldsymbol{x},\boldsymbol{s}) \quad (12)$$

In this banded formulation the RTE becomes

$$\boldsymbol{s}.\nabla I_j = k_j p_a\left[a_j(T) I_b(T) - I_j\right] \quad (13)$$

With the following boundary condition for a diffusive black wall:

$$I_{j,w} = a_j(T_w) I_b(T_w) \quad (14)$$

Note that the mean beam length approximation is now altogether avoided in the banded formulation. To calculate the incident radiation G and incident flux q''_{in}, Eq. (12) is simply substituted in Eq. (9) and Eq. (11). However the source term now takes this form:

$$\nabla.\dot{q}''_r(\boldsymbol{x}) = \sum_{j=0}^{J} \kappa_j(\boldsymbol{x}) p_a(\boldsymbol{x}) \left[4\pi a_j(\boldsymbol{x}) I_b(\boldsymbol{x}) - \sum_i \omega_i(\boldsymbol{x}) I_{i,j}(\boldsymbol{x},\boldsymbol{s})\right] \quad (15)$$

Where ω_i is the i^{th} solid angle. The original FireFOAM code for the finite volume solver (fvDOM) was modified accordingly by the present authors to accommodate for banded RTE solutions involving the WSGG weighting coefficient. The modification actually holds for any other type of banded RTE solution method, e.g. with a box model. It is worth noting that the absorption coefficients used in the WSGG model do not physically match the actual gas absorption coefficients, and moreover the actual gas spectral information cannot be recovered. The approach would be suitable in principle for radiative transfer in gases or gases/soot mixtures. For fire suppression by water sprays applications where the attenuation and emission by both the gas and liquid droplet phases should be accounted for, the WSGG is problematic because the droplets radiative properties are spectrally dependent and should be used with the physical gas absorption coefficient in spectral regions where both phases interact with the incident radiation. This is the motivation behind the development and assessment of a box model that will retain the actual physical value of the gas phase absorption coefficient.

2.4. Box model

In a box model, the absorption coefficient in each band forms a rectangular shape on the wavenumber spectrum, where the width $\Delta\eta_e$ is an equivalent bandwidth and the height κ is the constant absorption coefficient. Such a stepwise-grey approximation may be obtained from any band model [30]. In the present study the EWB was used to derive the box parameters from the band absorptance. For non-homogeneous cases, EWB correlations require an integration of transmissivity along an inhomogeneous optical path, hence in this work a Curtis-Godson scaling was applied for fire applications, as described in e.g. [31,32]. The main interest of using a box model over the spectral EWB is the significant computational gains resulting from using one physical absorption coefficient in each band of the absorbing/emitting gas. The drawback is the sensitivity of accuracy to equivalent bandwidth calculations [30]. In regular box models described in the radiation literature the values of $\Delta\eta_e$ are calculated on the fly during simulations; this could be prohibitive in terms of computing time. For the present work, the authors have fixed the band limits after an extensive sensitivity study of $\Delta\eta_e$ to temperature, path length and gas pressure [33]. This study shows that in the range of temperature, path length and pressure that is relevant for fire applications, bandwidths do not broaden as much as to cause many overlaps between bands from different gas species (unlike in oxy-fuel combustion, as seen in e.g. [34]). The bands that did frequently overlap were lumped together for maximum computational efficiency. More potential CPU gain was allowed by subsequently removing EWB band absorptance calculations from the modified box model, since those only serve to calculate the equivalent bandwidths. This modified box model then underwent testing under different radiation-only scenarios benchmarked by SNB data and turned out to work better than previous versions using on-the-fly bandwidth calculations [33]. The working band limits are thus as in Table 1, from which

the $\Delta\eta_e$ are easily obtained. The box (mass) absorption coefficient may then be obtained by e.g. Modest's correlation [30]:

$$\bar{\kappa} = \alpha/\Delta\eta_e \tag{16}$$

$$\alpha = \alpha_0 \frac{\Psi(T)}{\Psi(T_0)} \tag{17.a}$$

$$\alpha_{71\mu m} = 5.455\exp(-9\sqrt{T_0/T} - 1) \tag{17.b}$$

$$\alpha_{2.7\mu m} = \sum_{n=1}^{3} \alpha_n \tag{17.c}$$

Where α_0 is a tabulated EWB parameter obtained from e.g. [30]. For vibration-rotation bands (Eq. (17.a)) the non-dimensional function of temperature Ψ is obtained from the semi-tabulated correlations of Lallemant and Weber [35] which advantageously replace the complex expression of the original EWB formulation of Edwards [36]. For the pure rotational band of H_2O at 71μm Eq. (17.b) is also taken from [30] and is a slight refinement from Modak's original correlation [37]. Eq. (17.c) is the standard correlation for the triple overlap at 2.7μm in H_2O. In this implementation the 2.7μm band of CO_2 is added as well as it was found to almost always overlap with the three H_2O bands in the sensitivity study [33]. Finally, to further speed up calculations, three bands were removed from calculations due to their mostly insignificant contributions to radiation in fire conditions (the 960 and 1060cm^{-1} bands of CO_2 and the 7250cm^{-1} band of H_2O). In the end 6 bands are used for fire simulations, plus one clear band that accounts for all windows, which is thus only 2 or 3 extra bands from the non-grey WSGG. The form of the RTE is analogous to that of the banded WSGG, i.e.

$$\boldsymbol{s}.\nabla I_j = \bar{\kappa}_j \rho_j \left[\Delta F_j I_\mathrm{b}(T) - I_j\right] \tag{18}$$

Where

$$\Delta F = F(\lambda_U, T) - F(\lambda_L, T) \tag{19}$$

With F the fractional blackbody emission power. Similarly, for the boundary condition, this expression replaces the WSGG's $a(T)$ weight in Eq. (14), with T_w in place of T.

Table 1: Fixed band limits for the EWB-based box model

Band head location	Gas species	Bandwidth (μm)	Bandwidth (cm^{-1})
5350cm^{-1} or 1.87μm	H_2O, CO_2	1.8481-1.8907	5289-5411
3760cm^{-1} or 2.7μm	H_2O, CO_2	2.4907-2.8531	3505-4015
2410cm^{-1} or 4.3μm	CO_2	4.1494-4.5851	2181-2410
1600cm^{-1} or 6.3μm	H_2O	5.4885-7.2569	1378-1822
667cm^{-1} or 15μm	CO_2	13.3156-17.1821	582-751
140cm^{-1} or 71μm	H_2O	17.1821 - ∞	0 - 582

3. Results and discussion

3.1. Canonical case (two-dimensional enclosure)

This case scenario is from Goutiere et al. [9] and serves the purpose of assessing the accuracy of the new FireFOAM gas property models in a non-flowing, non-reactive environment. A rectangular, 1m x 0.5m enclosure with a 61 x 31 uniform Cartesian mesh and

cold black boundaries is filled with an inhomogeneous, non-isothermal CO_2 gas phase. The temperature and mole fraction distributions are governed by Eq. (20) and Eq. (21).

$$T(x,y) = T_0[0.3333(1-2|x-0.5|)(1-4|y-0.25|)+1] \quad (20)$$
$$c(x,y) = c_0[4(1-2|x-0.5|)(1-4|y-0.25|)+1] \quad (21)$$

Where T_0 = 1200K and c_0 = 0.02. The temperature varies between 1200 and 1600K (peak occurs in the central region). The mole fraction follows an analogous distribution and varies between 0.02 and 0.10 [9]. The incident radiative heat flux and the radiative source term are sampled along four lines, i.e. (x ,y = 0) and (x = 1, y) for the fluxes ; (x, y = 0.5) and (x = 0.5, y) for the source terms. The FireFOAM results from the grey, banded WSGG and box models are compared against the benchmark solution of [9] which is a ray-tracing method (RTM) combined with a SNB gas property model. A preliminary study was run with FireFOAM in ref. [33] to assess the accuracy of the FVM solver against the RTM used in [9] independently of any gas property model. This scenario used the same rectangular geometry and mesh with a uniform grey gas phase with κ = 0.5. The relative error between the FVM and the RTM of [9] overall turned out to remain under 3%, as long as a minimum of 16 solid angles were used in the FVM.

The Johansson WSGG model was left out as it does not handle single-species gases. The comparison is shown on Figure 1. It is immediately visible that the behaviours are better along the x axis than along the y axis, likely because the gas field variations are sharper along y. For the source term, the mean beam length approximation required by the grey WSGG models is likely responsible for the important discrepancies seen at the boundaries in both directions. Elsewhere, the grey models can show errors of up to 25-30% relative to the SNB solution. The banded WSGG models perform much better and also more consistently as in both directions the source term matches the SNB within 10-15%. For the incident flux, the banded models are always under 10% relative error. The grey WSGG does well along x (~12% difference) but much less so along y (up to 30% difference). The box model closely follows the banded WSGG trends (source term, flux alike) and even occasionally outperforms the WSGG in the central region (source term almost exactly matches the SNB), however the boundary effect can get slightly too pronounced in the source term. Overall, there is little difference between the Cassol and Smith versions of the WSGG. Rather, the differences seem induced by the implementation method (grey or banded).

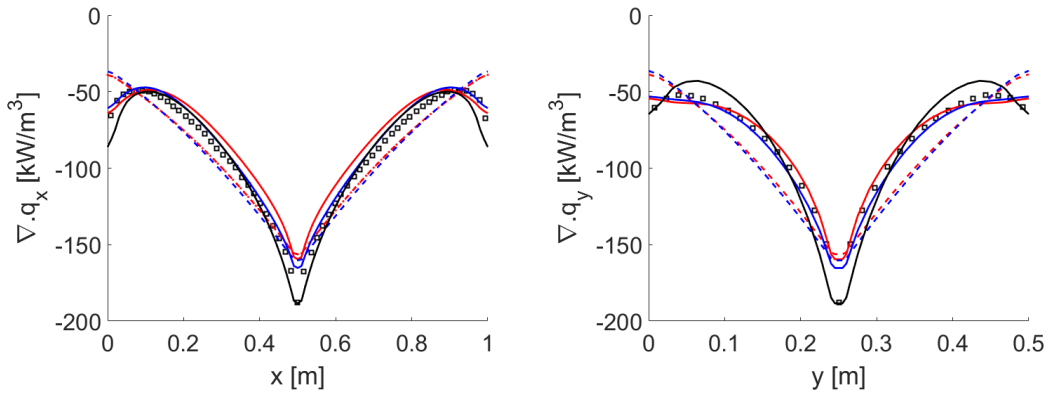

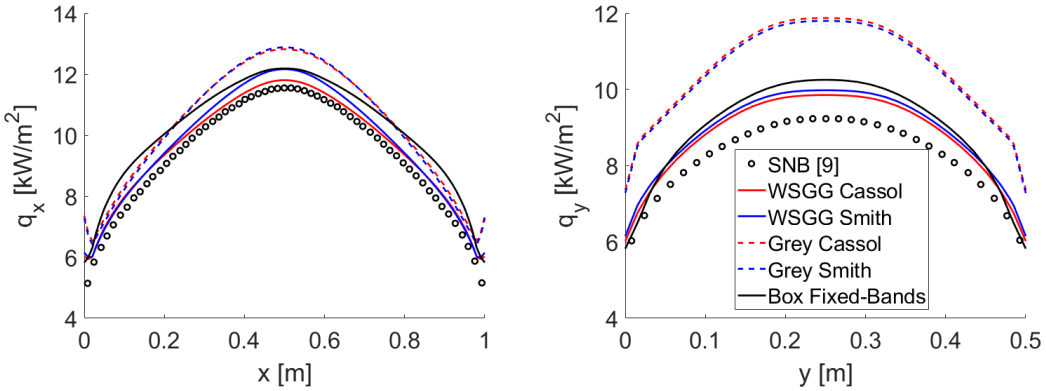

Fig. 1: FireFOAM (grey, WSGG, box models) vs SNB of [9] in the 2D canonical case of [42]. Top: radiative source term along (x, y = 0.25) and (x = 0.5, y), bottom: incident flux along (x, y = 0.5) and (x = 1, y)

3.2. Methanol pool fire

Canonical radiation scenarios are useful to validate a model implementation and quantify its accuracy in a controlled environment, but such studies are commonplace in the radiation literature. Radiation calculations in a fire simulation represent an entirely different challenge that encompasses several areas of physics. Prediction uncertainty can arise from key variables such as temperature, turbulent structures, flame shape, etc. One of the goals behind this body of work was to assess the practicality of non-grey gas property models in the context of CFD-LES simulated fires, as well as the accuracy. It is true that a proper quantitative analysis is difficult in light of the above-cited uncertainties, and the authors do acknowledge that the models used here are approximate ones and thus they cannot be expected to perfectly match e.g. a narrow band prediction. But, the authors believe that the implemented models should be deemed acceptable for CFD use if the error relative to the experimental radiation data is of the same magnitude as the one properly quantified in canonical radiation cases. The authors also feel that there are many studies already available that feature decoupled radiation calculations in synthetic fires (e.g. [6] or [11]), and that performing a similar study with FireFOAM would add little novelty from a typical canonical radiation scenario. Decoupled scenarios are convenient because they allow the generation of one's own benchmark data from detailed radiation modelling strategies, but it can be argued that the semi-empirical correlations used to rebuild the fields of temperature, soot, turbulence etc. do not eliminate 100% of the errors (centreline flame structure is correct, but elsewhere values can be seen to gradually move away from the experimental baseline). Moreover, FireFOAM was designed (and is already used) to handle potentially complex fire situations, rather than reproduce canonical test cases. It is aimed as much towards fire scientists as towards heat transfer engineers; a certain user-friendliness is desirable, which is better achieved when one can launch a fire simulation and obtain all the results in one go, rather than solving the flow field first, then radiation separately. The issue however is that fully coupled simulations with a detailed radiation model are too costly - hence the general idea of this work is based on a compromise between accuracy, cost and practicality. With that in mind, a non-grey radiation capability is desirable for the situations that may require it, but that does not mean traditional grey models should be

dismissed when they can give, not similar but at least comparable accuracy, for a fraction of the computing cost of a more detailed model.

On another hand, due to the flow field being resolved, chances are that these gas property models (grey/banded WSGG and box models) may behave differently in a "real" fire simulation, compared with canonical cases or synthetic fires. Such a study has not yet been undertaken to the best knowledge of this author, and it is thus believed that the results of this work will provide a valuable step towards more practical fire engineering scenarios such as the example above.

The benchmark data for this work are taken from the experiments of Klassen and Gore [4] who measured temperature, soot volume fractions and radiative heat transfer in pool fires of different fuels and sizes. Their data for the soot-free 30cm methanol fire provides an ideal ground for a comparative study of gas phase radiation models such as the WSGG and the EWB-box model. The flux was measured both radially at the pool surface (r, z = 0) and vertically (r = 82.5cm, z), where the origin ($r = 0$, $z = 0$) is the centre of the pool surface. The reference temperature and velocity data are taken from Weckman and Strong [38], whose 30cm methanol fire setup is close to that of [4]. Temperatures for fires of different sizes/heat release rate (HRR) may be compared using the scaling technique of McCaffrey [39], although the difference is only a few kilowatts between [4] and [38]. The 1cm wider burner in [38] is not expected to have any visible influence. The taller burner lip height of [4] was initially reproduced in early simulations, but eventually was dropped for its lack of impact on the predicted flame structure. Both experiments were conducted in quiescent environments ensuring no crosswind may have altered the flame shape. For the transducer measurements of the radiant heat flux, Klassen and Gore report an uncertainty inferior to ±15% at flame steady state [4].

The working steps for this study were as follows. First, grid tests were run until the time-mean centreline temperature and velocity profiles converged with one another and agreed well enough with the measurements of [38]. After finding an appropriate grid size, the second step was to calibrate the TRI parameters with a default gas radiation model (for convenience, the Smith WSGG henceforth), with successive simulations until the total radiant fraction (Xr) agreed with the experimental data of [4]. That agreement did not have to be perfect, since between the gas radiation models the total radiant output was expected to vary anyway (reasonably, i.e. within a few percents). Thus, for the comparisons of radiant heat fluxes, six final simulations were run comprising the two grey and three banded WSGG models and the EWB-box model. For clarity, the models will be referred to as "WSGG Smith", "WSGG Cassol", "WSGG Johansson" for the banded WSGG solutions, and "Grey Smith", "Grey Cassol" (grey WSGG solutions) and "Box Fixed-Bands". The grey WSGG calculations were based on the total emissivity calculations from a mean beam length (MBL). The integral length scale [24] was used for MBL calculations, i.e. $S = \left(Q/T_\infty \rho_\infty Cp_\infty \sqrt{g}\right)^{0.4}$, instead of the more usual correlation $S = 3.6V/A$, because the volume and area of the flame zone may be difficult to estimate from e.g. cylindrical or conical approximations of the actual flame shape.

Each simulation was run for 30 seconds, with time-averaging starting after 8 seconds, long after the flame has developed to its full scale. The domain is an O-grid based cylinder of radius R = 82.5cm and height H = 1.2m, with grid nodes clustering towards the fuel inlet at the bottom (pool centre at r = 0, z = 0). The heat release rate is not a prescribed input parameter, but controlled by the user-specified mass flow rate. Hence in this work the correct HRR is obtained by feeding the fuel inlet at a constant methanol mass flow rate of 0.1069g/s at boiling point temperature, i.e. 338K. One may note that physically speaking those are liquid fuels, treated as surface boundaries in the simulation, hence only the gas phase is being resolved (no need for pyrolysis modelling unlike with solid fuels). Ignition is immediate, as ensured by the infinitely fast chemistry LES-EDC model, and the combustion reaction is driven by a single equation. The other boundaries are open, set to 300K and all are black. Detailed LES parameters may be found in [23,24] for the same fuel.

3.2.1. Simulation parameters and CPU times

Radiation parameters were set for maximum CPU efficiency as follows: maximum number of solver iterations = 1 (that is, the FVM solver; not to be mistaken with the Geometric Agglomerated Algebraic Multigrid or GAMG algorithm which solves an RTE per solid angle and spectral interval), convergence criterion = 10^{-4}, solver frequency = every 30 time steps. A preliminary study showed that the non-scattering RTE converges easily (3-4 iterations of the GAMG solver, out of a possible 1000), being a simple 1st order difference equation, thus much CPU time can be saved by minimising the solver iterations. Besides, radiation propagates at light speed, and with a constant time step of 5.10^{-4} seconds the flame structure does not change significantly enough to justify a radiation update at every time step (frequency is set to 30 time steps instead). On another hand, every time radiation is updated, FireFOAM solves a number of transfer equations, which is the product of the number of solid angles N_{ang} and the number of spectral bands/grey gases N_{bands}. The latter is fixed by the gas property model, e.g. for a grey property model, N_{bands} = 1, and for a banded WSGG, N_{bands} = 4 or 5. But N_{ang} has to be adjusted depending on the severity of ray effects in a particular case. For this work N_{ang} had to be set to 600, because the radiant flux data was otherwise unusable from too much numerical distortion. Hence, with a grey model 1 x 600 equations are solved every radiation update, respectively 4 x 600 with the Smith WSGG model, and so forth. This turned out to have a significant impact on the total computing times, summarised in Table 2: a full fire simulation is roughly 3-4 times slower when using a banded model.

Table 2: CPU time of 30cm methanol fire simulations (0 to 30s) with 600 solid angles for the various gas radiation model studied

Radiation model	Number of bands	CPU time
Grey Smith	1	(ref.)
Grey Cassol	1	x1.1
WSGG Smith	4	x2.9
WSGG Cassol or Johansson	5	x3.4

Box model "Fixed Bands"	7	x4.3

3.2.2. Grid independence and effect on temperature prediction

Five grids were tested, of respective smallest cell sizes (in millimetres): 11.6, 10.1, 9.3, 8.5, 8.0mm, labelled "grid #1" (coarsest) to "grid #5" (finest). The default gas radiation model for these runs is the WSGG Smith. Apparent grid independence was achieved by grid #3, since #4 and #5 yielded very similar mean temperature and velocity profiles (Figure 2), hence for the rest of this study grid #3 is used. The scaling techniques of McCaffrey are used (with Q the total heat release rate and $Uz^* = Uz/Q^{0.2}$) to verify that the overall flame structure does exhibit the three zones, i.e. continuous, intermittent and thermal plume. In the continuous flame zone ($z/Q^{0.4} < 0.08$), simulated temperatures are between the McCaffrey model correlations and Weckman and Strong's measurements, some 100K from either baseline. This result is not surprising as other FireFOAM contributors reported the same trend in [19,24], interpreting the underpredictive trend in lower regions as an intrinsic limitation of the combustion model due to relatively low Reynolds numbers at the bottom of the flame. The upper regions (intermittent flame and thermal plume) agree quite well with the experimental data points and should be accurate enough for the subsequent radiative flux comparisons. Radial temperature profiles for grid#3 and subsequent also show good overall agreement (Figure 3), despite the fact that temperatures drop quicker than they should away from the central axis ("necking" phenomenon).

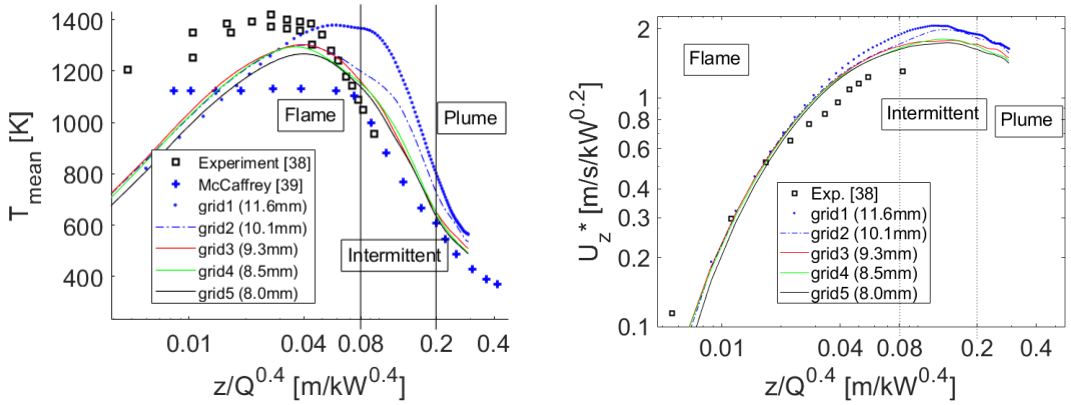

Fig. 2: Grid sensitivity of centreline mean temperature and velocity

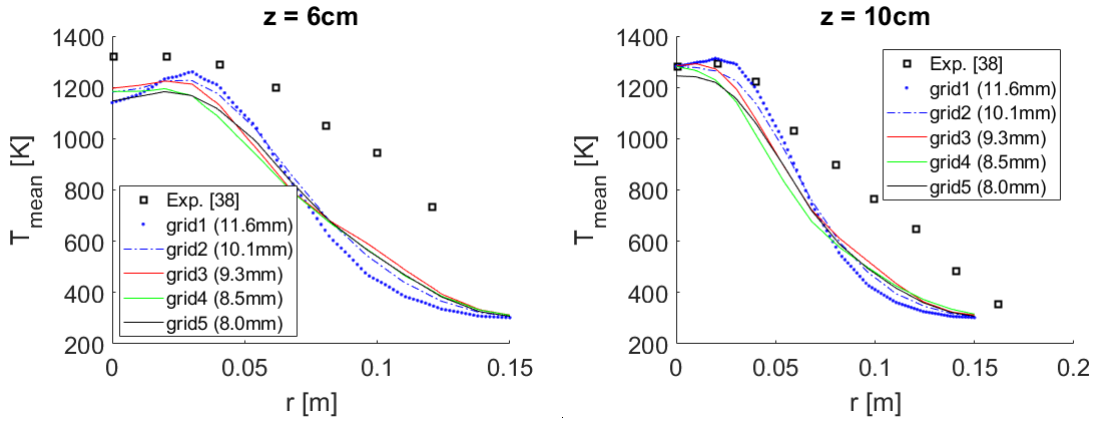

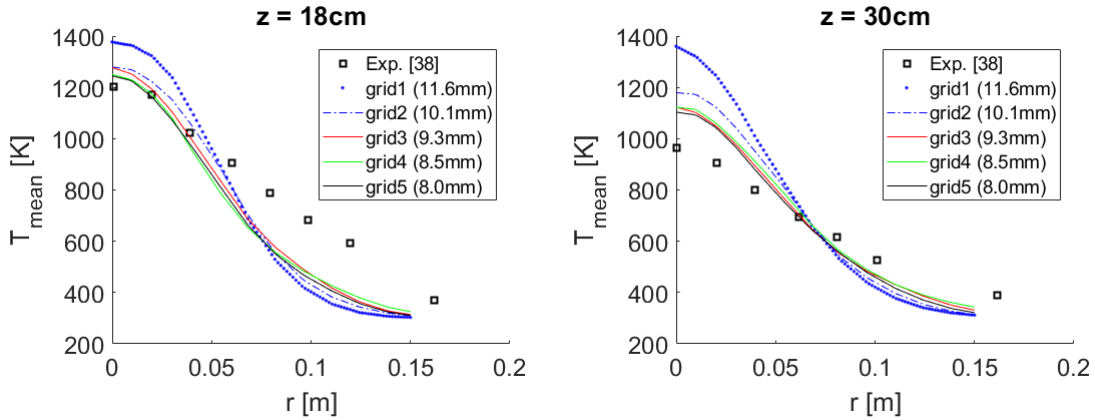

Fig. 3: Grid sensitivity of radial temperature at different elevations from pool (*z* = 0)

3.2.3. Influence of TRI parameters

The TRI parameter C_{TRI} appears in Eq. (5b). The C in Eq. (6a) is not a TRI parameter but it impacts how the turbulent temperature fluctuation is modelled, which in turn impacts Eq. (5b). A trivial combination of these equations shows that radiation calculations are driven by the product C x C_{TRI}. After some trial and error, it was found that the right radiation fraction was likely to be obtained with C x C_{TRI} ~ 3.5 (Fig. 4). Besides, one may note that the correlation is almost linear. The calibration was done with the Smith WSGG, which somewhat biases the comparative study in favour of that model, hence why the relative differences are more interesting here, although the other models turned out to behave very closely as a whole. On another hand, only C plays a role in the modelled component of T_{RMS}. Fellow FireFOAM workers used C ~ 2 and 1.25 < C_{TRI} < 2.5 for their 30cm heptane case in [19], but for the methanol fire this results in too high T_{RMS}, (Weckman and Strong's data [38] is in the 400K range, some 200K lower than the heptane fire). But, it was also learned from preliminary runs that the pool surface radiant flux (where turbulence is present) is always too low without a TRI correction. After some trial and error, it was found that the results were best with C = 0.25 and C_{TRI} = 14. Predictably, other sets of constants with the same CxC_{TRI} product yielded similar radiation predictions (e.g., C = 0.5 and C_{TRI} = 7, or C = 2 and C_{TRI} = 1.75). Hence, the logic here is that a smaller C prevents overprediction of T_{RMS} while a larger C_{TRI} acts as a compensator. Still, it may be noted that T_{rms} can be overpredicted locally by some 100-150K (Fig. 5). This results however compares with other FireFOAM studies, e.g. [19] or [23] and the localised discrepancies may be inherent to FireFOAM itself.

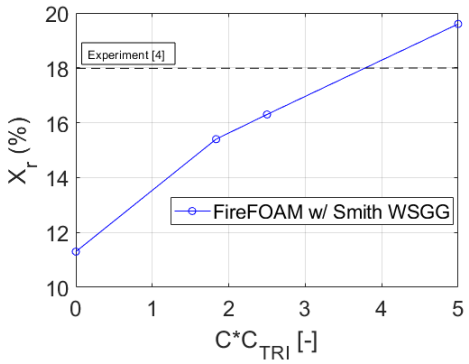

Fig. 4: Radiant fraction of the 30cm methanol fire as a function of C x C_{TRI}

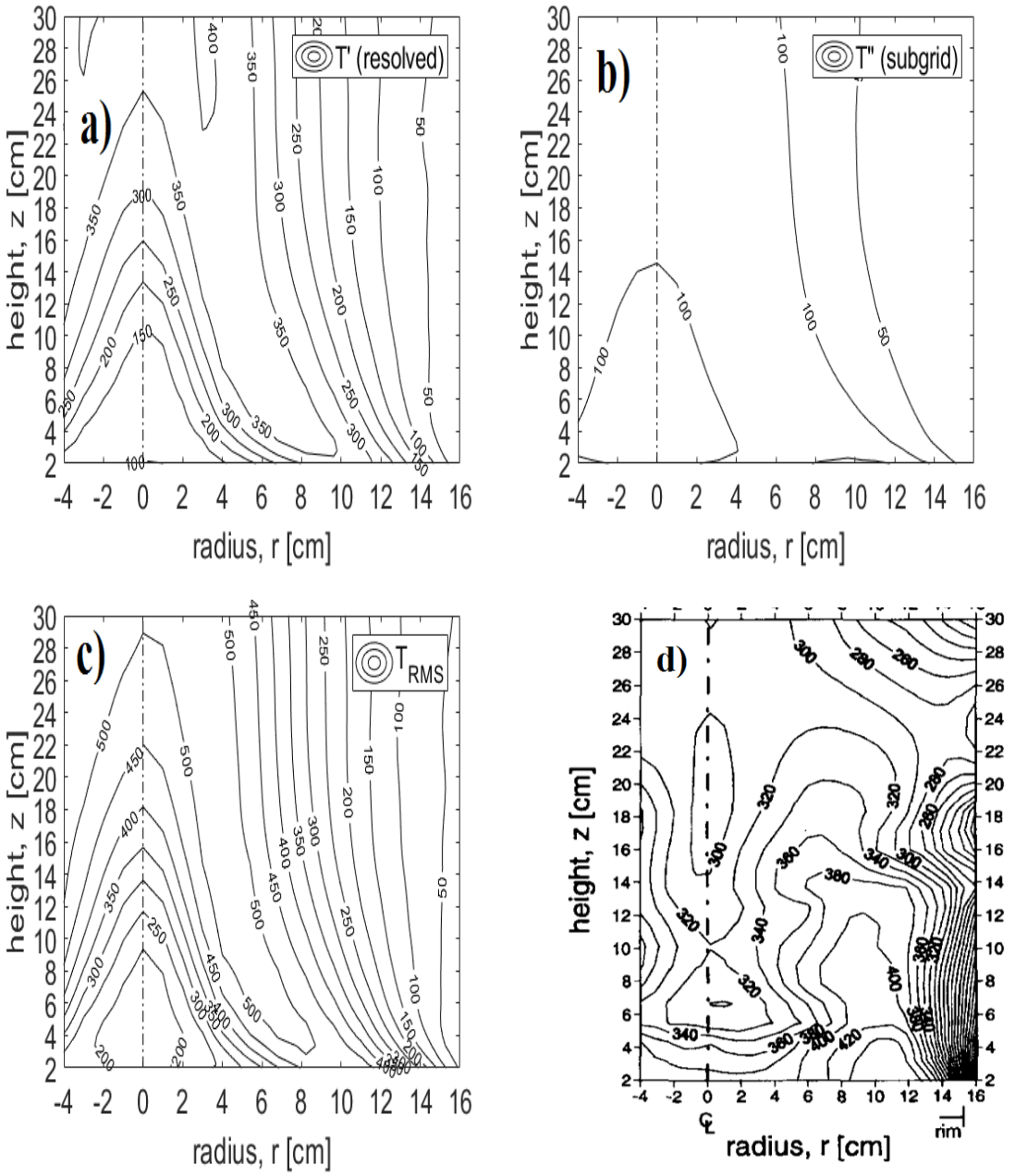

Fig. 5: Temperature fluctuation at steady state, top left to bottom right: resolved $\widetilde{T'}$ (a), subgrid $\widetilde{T''}$ (b), $\widetilde{T_{rms}} = \widetilde{T''} + \widetilde{T'}$ (c), experimental T_{rms} from [38] (d)

The methanol flame simulated here yielded an average optical thickness of ~0.1, based on calculations of the Planck-mean absorption coefficient at post-processing stage (the mean beam length is the integral length scale defined earlier). Furthermore, the contour plots on Figure 6 show that while not negligible, the absorption component of the source term is 1-2 orders of magnitude smaller than the blackbody emission term. The medium is thus optically thin which confirms the hypothesis made in section 2.2. Of course the optically thin approximation could have replaced the more involved FVM for radiation calculations, but the goal is for CFD engineers to be able to use the FVM for any fire scenario without prior knowledge of the radiative properties of the fire. As expected, the radiation source term is completely dependent on how well T_f is modelled. Immediately above the pool edge, the temperature self-correlation R_T^4 is 3 or 4 times more important than in the rest of the flame zone (Figure 7). This very much impacts the radiant source term which in the same region is increased roughly tenfold from the simulation with neglected TRI (Figure 8). In turn, the radiant flux too is affected at the bottom boundary (Figure 9): instead of peaking at the pool centre like the experimental points, the predicted flux indeed rises slightly some 8-10cm from the centre, before collapsing sharply nearer the pool edge This however remains a positive result, because without any TRI correction the flux is much too low at any radial position (nearly half the experimental values). The spatial distribution of the radiant flux may not be perfect, but the TRI corrections employed here do bring the overall feedback back to acceptable levels (including in the pool centre, where the flux is almost doubled from the C_{TRI} = 0 case). This qualitative agreement may be improved upon with some fine tuning on the modelling of T''.

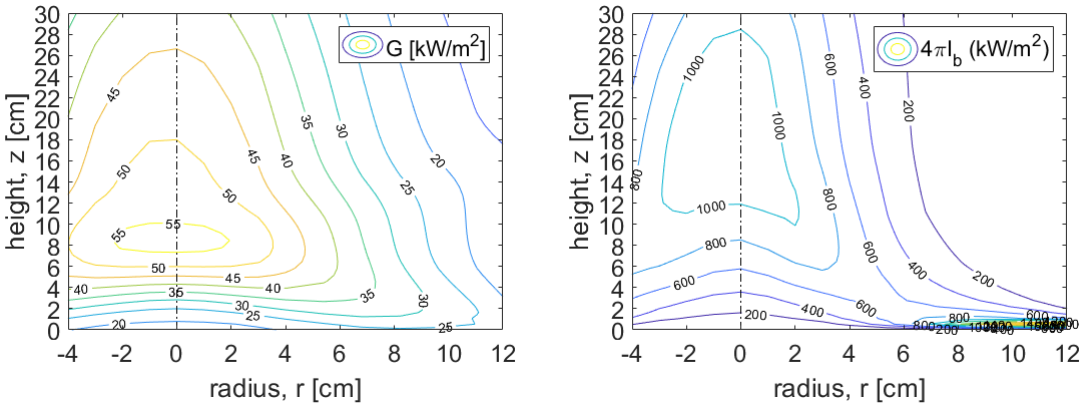

Fig. 6: Contours of absorption and emission terms of Eq. (10) at steady state

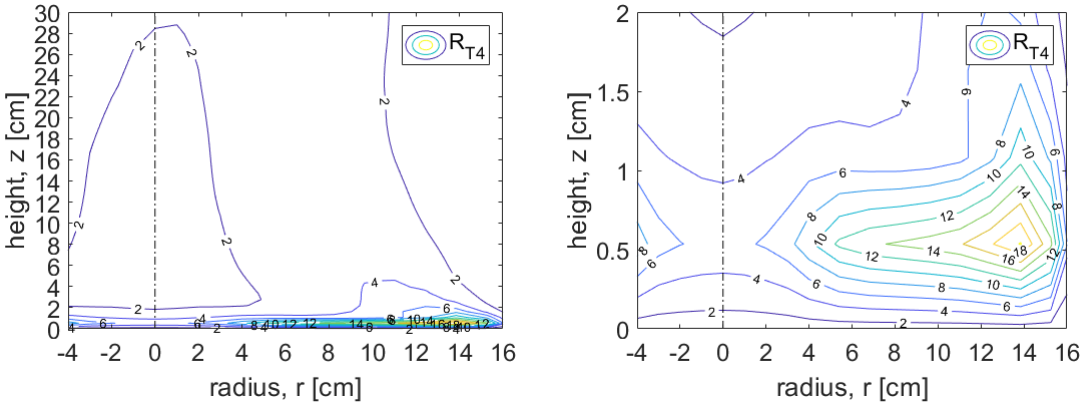

Fig. 7: Contours of temperature self-correlation R_T^4 at steady state

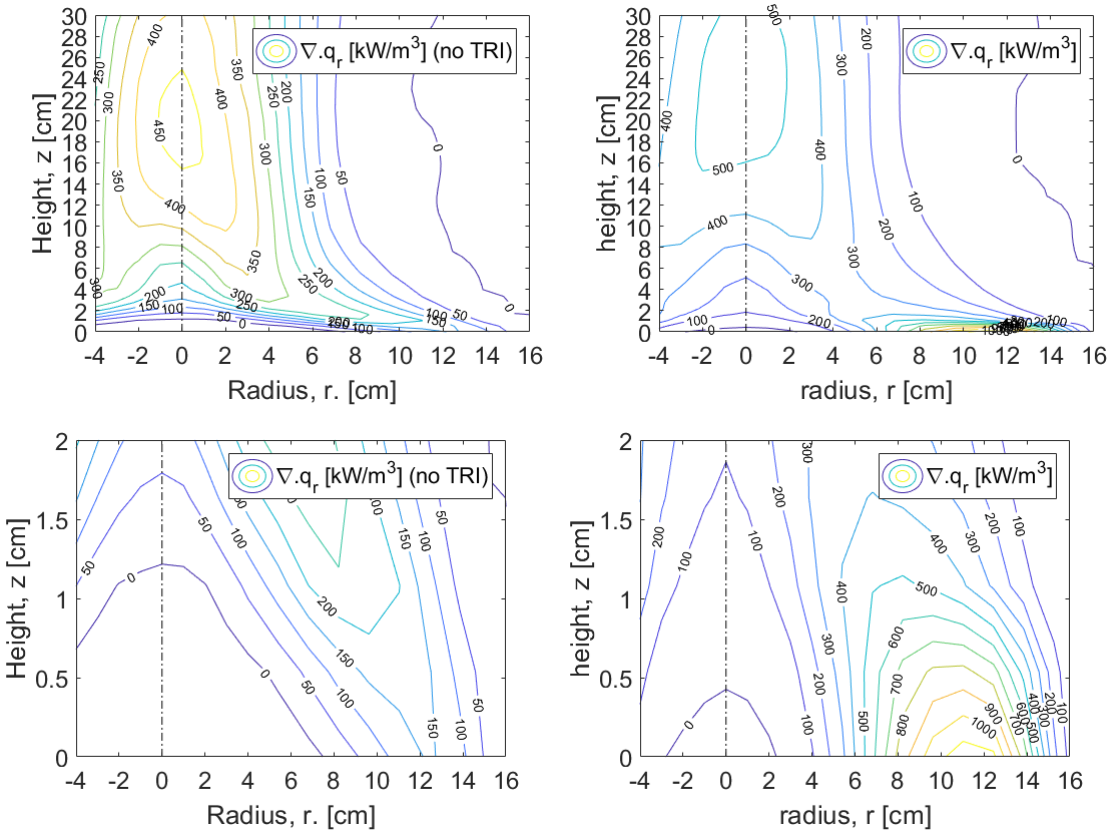

Fig. 8: Contours of radiant source term at steady state with and without TRI

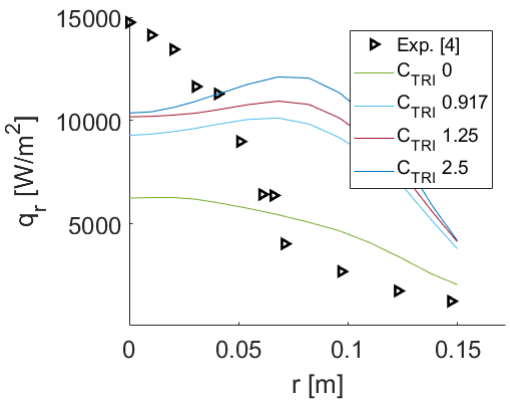

Fig. 9: Radiant feedback to pool surface (*z = 0*) with different TRI corrections

3.2.4. Comparison of gas radiation approaches

Figure 10 presents the centreline mean temperature predictions for the different gas modelling approaches. The results show that the effect of the gas radiation models on temperature is not significant for this particular flame with a maximum difference of 60K between all simulations and along the centreline. This relates to *Xr* variations of 2-3%. The total radiant fractions from the grey or banded WSGG models are very close and about 5% below the experimental value (Table 3), whereas the box model overpredicts the total power by a few percents. The spatial distribution of radiant energy reflects this result, in that the vertical flux is slightly overpredicted by the box model, and underpredicted by the other models, i.e. within 100W/m² at the power peak (Figure 10). Consistently with the findings of [11] in synthetic fires, the grey models project less radiant energy towards the far field. At a radial distance of 82.5cm from the pool centre, the radiant flux echoes the quality of temperature prediction inside the flame (axially), i.e. underpredicted inside the continuous flame zone and slightly overpredicted higher up. As to which gas radiation model to use, the choice may be dictated by practicality. The advantage of using the more CPU expensive Johansson WSGG model is not obvious here, since the cheaper Smith WSGG model has a ready set of absorption coefficients and emission weights for this particular stoichiometric ratio of water vapour and carbon dioxide. The Cassol WSGG is very similar to the other two in its performance, and also slower than the Smith model. Grey approximations are far from being irrelevant here and may be appreciated for their CPU efficiency. This relatively decent accuracy is likely due to the relative lack of severe temperature variations in comparison with environments such as oxy-fuel combustors. Also, this was a simple case where the mean beam length could be estimated without difficulties (the grey WSGG is MBL-sensitive, but strictly speaking Beer's law only holds for a spectral RTE solution, not grey or band-averaged methods). Besides, the MBL remains constant over time as soon as the flame has developed to its full scale. For transient problems e.g. spreading fires, a banded WSGG model is definitely more interesting as it requires no mean beam length specification. Finally, some small, residual ray effect is seen in the vertical flux of Figure 11, near the bottom where cells are the smallest. The angular space between the XY plane and the domain's axis was discretised with as many as 50 angles. Further resolution increase (up to 90 angles) produced negligible improvement on ray effects, not worth the much increased computational effort.

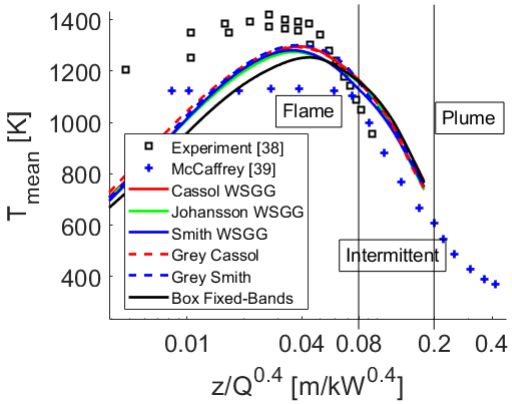

Fig. 10: Centreline mean temperatures from 6 gas radiation models

Table 3: Comparison of radiant fractions

	Radiant fraction X_r (%)
Experiment [4]	18
Grey Smith	17.2
Grey Cassol	16.7
Smith WSGG	17.2
Cassol WSGG	16.8
Johansson WSGG	17.3
Box Fixed-Bands	21.6

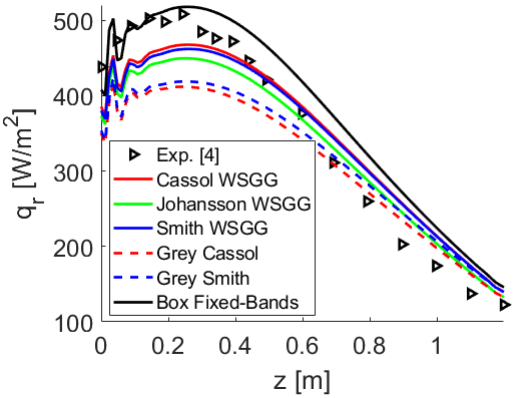

Fig. 11: Vertical radiant flux along (*r* = 82.5cm, *z*) from 6 gas radiation models

4. Conclusion

The 30cm methanol pool fire of Klassen and Gore [4] and Weckman and Strong [38] was simulated with the open-source LES code FireFOAM, based on an FVM radiation solver. The authors upgraded the radiation capability to non-grey models and added five different implementations of the WSGG (two grey, three banded) and an EWB-based box model specifically optimised for fire simulations and CPU efficiency. Analysis of the radiant fluxes showed that the newer WSGG correlations of Cassol et al. and Johansson et al. were found to yield no significant differences with the older model by Smith et al. for the simulated pool fire. It could be argued that this statement may not be generalised since it is based on limited experimental data, and the influence of the non-radiative modelling assumptions may overshadow the differences in the gas property models; but the canonical radiation case scenario showed the same trend, as did a number of variants not shown here but studied in [33]. Anyhow, for this particular case, the authors recommend using the Smith WSGG as it was 15-20% faster than the more recent models. The Johansson model will be interesting for fire simulations where the mole fraction ratio of water vapour and carbon dioxide varies from 1 or 2, or cannot be determined beforehand (e.g. complex fuels). Grey implementations of these models are 3 times faster, but this large difference is much due to the higher number of

solid angles employed here (600) to minimise the ray effects (because grey models then involve 600 directional RTE solutions, whereas banded models involve 600 x N_{bands} solutions). Overall, grey models managed to handle the gas medium's non-uniformities quite well, but they underpredicted the radiant fluxes and the total radiant output. If a mean beam length cannot be calculated trivially, then a banded WSGG model is recommendable for fire simulations. The EWB-derived box model, optimised for maximum CPU efficiency, turned quite capable of matching a banded WSGG (less than 30% slower), although it did slightly overpredict the total radiant output. Overall, all models managed to reproduce the experimental radiant fluxes well, except at the fuel inlet centre where radiant power peaks. TRI modelling also showed a significant effect on the overall radiant energy yield, which can become very strong locally (e.g. just above the burner surface), but that difference is only really important between no TRI and any TRI modelling, as the increasing of TRI effects did not make a significant difference on the radiant flux. However, the distribution of the pool surface flux is very sensitive to how the turbulent temperature fluctuation is estimated, which may require improvement. Due to the experimental RMS temperatures being fairly low (around 400K), in this work the subgrid component of T_{rms} benefitted from being kept less than half the resolved component. In future works the box model will be coupled with a non-grey Mie theory model for radiation calculations in simulated fires suppressed with water sprays (non-grey WSGG models cannot be coupled to a non-grey Mie model).

5. Acknowledgements

The authors wish to thank FM Global for their financial and technical support.

6. References

[1] Chan SH. Combined Radiation and Combustion. In: Tien CL, editor. Annual Review of Heat Transfer, Begell House, New York and Redding, CT, 2005, vol. 14, p. 49-64.
[2] Viskanta R. Radiative Transfer in Combustion Systems: Fundamentals and Applications. Begell House, New York and Redding, CT; 2005.
[3] Hamins A, Kashiwagi T, Buch RR. Characteristics of pool fire burning, Fire Resistance of Industrial Fluids. Proceedings ASTM STP 1284. June 20, 1995, ASTM PCN 04-012840-12. (1996) 15-41.
[4] Klassen ME, Gore JP, Structure and radiation properties of pool fires, Final Report NIST-GCR-94-651. (1994) 153.
[5] Wakatsuki K, Jackson GS, Hamins A, Nyden MR, Effects of fuel absorption on radiative heat transfer in methanol pool fires, Proc. Combust. Inst. 2007; 31:2573-80.
[6] Consalvi JL, Liu F, Radiative transfer in the core of axisymmetric pool fires - I: evaluation of approximate radiative property models, Int. J. Thermal Sciences. 2014;84:104-17.
[7] Radiation heat transfer in OpenFOAM, Göteborg, Chalmers University of Technology, 10.12.2009
[8] Coelho PJ, Numerical simulation of radiative heat transfer from non-gray gases in three-dimensional enclosures, J. Quant. Spectrosc. Radiat. Transfer. 2002;74:307-28.

[9] Goutière V, Liu F, Charette A, An assessment of real-gas modelling in 2D enclosures, J. Quant. Spectrosc. Radiat. Transfer. 2000;64:299-326.
[10] Bressloff NW, The influence of soot loading on weighted sum of grey gases solutions to the radiative transfer equation across mixtures of gases and soot, Int. J. Heat Mass Transfer. 1999;42:3469-80.
[11] Krishnamoorthy G, A comparison of gray and non-gray modeling approaches to radiative transfer in pool fire simulations, J. of Hazardous Materials 2010;182:570-80.
[12] Consalvi JL, Demarco R, Fuentes A, Melis S, Vantelon JP, On the modeling of radiative heat transfer in laboratory-scale pool fires, Fire Safety J. 2013;60:73-81.
[13] Dembele S, Wen JX, Assessment of spectral narrow band and global gas radiation models for computational fluid dynamics simulations of pool fires, Numerical Heat Transfer - Part B: Fundamentals 2003;44(4):365-85.
[14] Cumber PS, Fairweather M, Ledin HS, Application of wide band radiation models to non-homogeneous combustion systems, Int. J. Heat Mass Transfer 1998;41(11) :1573-84.
[15] Cumber PS, Fairweather M, Evaluation of flame emission models combined with the discrete transfer method for combustion system simulation, Int. J. Heat Mass Transfer 2005;48:5221-39.
[16] Hostikka S, Mcgrattan KB, Hamins A, Numerical Modeling of Pool Fires Using LES and Finite Volume Method for Radiation, Fire Safety Science 2003;7:383-94.
[17] Hottel HC, Sarofim AF, Radiative Transfer, New-York: McGraw-Hill; 1967.
[18] Chen Z, Wen J, Xu B, Dembele S, Extension of the eddy dissipation concept and smoke point soot model to the LES frame for fire simulations, Fire Safety J. 2014;64:12-26.
[19] Chaterjee P, Wang Y, Meredith KV, Dorofeev S, Application of a subgrid soot-radiation model in the numerical simulation of a heptane pool fire, Proc. Combustion Instit. 2015;35:2573-80.
[20] Wu B, Zhao X, Roy SP, The radiative interactions between nongrey gas, soot, water mist and turbulence: a Monte Carlo ray tracing study, 9th Open Source CFD Fire Modeling Workshop, Norwood MA, USA, May 9-10, 2017.
[21] Meredith KV, Zhou X, Ebrahimzadeh S, Merci B, Numerical simulation of spray-plume interactions, 9th U. S. National Combustion Meeting Organized by the Central States Section of the Combustion Institute May 17-20, 2015 Cincinnati, Ohio.
[22] Magnussen BF, Hjertager BH, Development of the eddy-break-up model of turbulent combustion, Proc. Combust. Inst. 1976;16:719-29.
[23] Chen Z, Wen J, Xu B, Dembele S, Large eddy simulation of a medium-scale methanol pool fire using the extended eddy dissipation concept, Int. J. Heat Mass Transfer 2014;70:389-408.
[24] Chen ZB, Extension of the eddy dissipation concept and laminar smoke point soot model to the large eddy simulation of fire dynamics, PhD thesis, Kingston University London, UK, 2012.
[25] OpenFOAM Users' Guide, OpenCFD Ltd, Bracknell, UK, 2011.
[26] Smith TF, Shen ZF, Friedman JN, Evaluation of coefficients for the weighted sum of gray gases model, ASME J. Heat Transfer 1982;104(4):602–8.

[27] Cassol F, Brittes R, Franca FHR, Ezekoye OA, Application of the weighted-sum-of-gray-gases model for media composed of arbitrary compositions of H_2O, CO_2 and soot, Int. J. Heat Mass Transfer 2014;79: 796–806.
[28] Johansson R, Leckner B, Andersson K, Johnsson F, Account for variations in the H_2O to CO_2 molar ratio when modelling gaseous radiative heat transfer with the weighted-sum-of-grey-gases model, Combust. Flame 2011; 158(5):893-901.
[29] Modest MF, The weighted-sum-of-gray-gases model for arbitrary solution methods in radiative transfer, J. Heat Transfer 1993; 113:650-6.
[30] Modest MF. Radiative Heat Transfer. Third ed. New-York: Academic Press; 2013.
[31] Chan SH, Tien CL, Total band absorptance of non-isothermal infrared-radiating gases, J. of Quantitative Spectroscopy and Radiative Transfer 1969;9(9):1261–71.
[32] Cess RD, Wang LS, A band absorptance formulation for nonisothermal gaseous radiation, Int. J. Heat and Mass Transfer 1970;13:547-55.
[33] Sikic I, Radiative heat transfer for modelling fire and fire suppression, PhD thesis, University of Warwick, Coventry, UK, 2018.
[34] Marzouk OA, Huckaby ED. Nongray EWB and WSGG Radiation Modeling in Oxy-Fuel Environments. In: Zhu, J editor. Computational Simulations and Applications, Rijeka, Croatia: InTech; 2011.
[35] Lallemant N, Weber R, A computationally efficient procedure for calculating gas radiative properties using the exponential wide band model, Int. J. Heat and Mass Transfer1996;30(15):3273-86.
[36] Edwards DK, Absorption of radiation by carbon monoxide gas according to the exponential wide-band model, Appl. Optics 1965;4(10):1352-53.
[37] Modak AT, Exponential wide band parameters for pure rotational band of water vapor, J. Quant. Spectrosc. Radiat. Transfer 1978;21:131-42.
[38] Weckman EJ, Strong AB, Experimental investigation of the turbulence structure of medium-scale methanol pool fires, Combustion and Flame 1996;105(3):245-66.
[39] McCaffrey BJ, Purely buoyant diffusion flames: some experimental results, Report NBSIR-79-1910, Washington D.C., 1979.
[40] Coelho PJ, Numerical simulation of the interaction between turbulence and radiation in reactive flows, Progress in Energy and Combustion Science 2007;33:311-83.
[41] Snegirev AY, Statistical modeling of thermal radiation transfer in buoyant turbulent diffusion flames, Combustion and Flame 2004;13651-71.